Springer Series in Advanced Microelectronics 13

Horst Zimmermann

Silicon Optoelectronic Integrated Circuits

Second Edition

Springer

Springer Series in Advanced Microelectronics

Volume 13

Series editors

Kukjin Chun, Department of Electrical and Computer Engineering, Seoul National University, Seoul, Korea (Republic of)
Kiyoo Itoh, Hitachi (Japan), Tokyo, Japan
Thomas H. Lee, Department of Electrical Engineering, CIS-205, Stanford University, Stanford, CA, USA
Rino Micheloni, PMC-Sierra, Vimercate (MB), Italy
Takayasu Sakurai, The University of Tokyo, Tokyo, Japan
Willy M. C. Sansen, ESAT-MICAS, Katholieke Universiteit Leuven, Leuven, Belgium
Doris Schmitt-Landsiedel, Lehrstuhl für Technische Elektronik, Technische Universität München, München, Germany

The *Springer Series in Advanced Microelectronics* provides systematic information on all the topics relevant for the design, processing, and manufacturing of microelectronic devices. The books, each prepared by leading researchers or engineers in their fields, cover the basic and advanced aspects of topics such as wafer processing, materials, device design, device technologies, circuit design, VLSI implementation, and sub-system technology. The series forms a bridge between physics and engineering, therefore the volumes will appeal to practicing engineers as well as research scientists.

More information about this series at http://www.springer.com/series/4076

Horst Zimmermann

Silicon Optoelectronic Integrated Circuits

Second Edition

Horst Zimmermann
EMCE
Technische Universität Wien
Vienna, Austria

ISSN 1437-0387 ISSN 2197-6643 (electronic)
Springer Series in Advanced Microelectronics
ISBN 978-3-030-05821-0 ISBN 978-3-030-05822-7 (eBook)
https://doi.org/10.1007/978-3-030-05822-7

Library of Congress Control Number: 2018964046

1st edition: © Springer-Verlag Berlin Heidelberg 2004 (Originally published by Springer-Verlag Berlin Heidelberg New York in 2004)
2nd edition: © Springer Nature Switzerland AG 2018
This work is subject to copyright. All rights are reserved by the Publisher, whether the whole or part of the material is concerned, specifically the rights of translation, reprinting, reuse of illustrations, recitation, broadcasting, reproduction on microfilms or in any other physical way, and transmission or information storage and retrieval, electronic adaptation, computer software, or by similar or dissimilar methodology now known or hereafter developed.
The use of general descriptive names, registered names, trademarks, service marks, etc. in this publication does not imply, even in the absence of a specific statement, that such names are exempt from the relevant protective laws and regulations and therefore free for general use.
The publisher, the authors and the editors are safe to assume that the advice and information in this book are believed to be true and accurate at the date of publication. Neither the publisher nor the authors or the editors give a warranty, express or implied, with respect to the material contained herein or for any errors or omissions that may have been made. The publisher remains neutral with regard to jurisdictional claims in published maps and institutional affiliations.

This Springer imprint is published by the registered company Springer Nature Switzerland AG
The registered company address is: Gewerbestrasse 11, 6330 Cham, Switzerland

Preface to the Second Edition

Since the first edition of this book in 2004, a huge amount of very interesting integrated optoelectronic devices and circuits were investigated and introduced in numerous publications. Therefore, Springer and I decided to publish this extended edition. Hot topics were integrated avalanche photodiodes, and there even was a hype on single-photon avalanche diodes (SPADs) and on SPAD sensor and imager ICs in the last decade. It was only possible to select some, which seemed to be kind of key publications to me. Optical wireless communication was improved by integrated avalanche photodiodes in the linear mode. In addition, first SPAD optical receivers eliminating electronic noise and trying to approach the quantum limit set by photon statistics had to be included. First, OWC experiments with SPAD receivers seem also to be worth of inclusion in this extended edition.

There was also considerable progress with the so-called silicon photonics foundry. Therefore, a chapter describing several advanced electronic-photonic integrated ICs was added.

There were also innovative pin photodiode OEICs introducing new circuit architectures for transimpedance and bandwidth enhancement. Furthermore, really astonishing high-pixel-count image sensors and three-dimensionally integrated image sensors had to be included.

I would like to thank Dr. Claus Ascheron from Springer for initiating this extended edition and his team for technical support with the text processor. From my current research group at TU Wien, I have to thank especially Dr. Michael Hofbauer, Dr. Bernhard Goll, Dr. Kerstin Schneider-Hornstein, Dr. Hiwa Mahmoudi, Bernhard Steindl, Dinka Milovancev, and Nemanja Vokic for their excellent work and strong motivation. In the same amount, I have to thank the former group members Dr. Paul Brandl, Dr. Tomislav Jukic, Dr. Nicola Zecevic, Dr. Robert Swoboda, Dr. Reinhard Enne, Wolfgang Gaberl, Dr. Milos Davidovic, Dr. Michael Förtsch, Dr. Mohamed Atef, Dr. Christoph Seidl, Dr. Johannes Knorr, Dr. Stefan Schidl, Dr. Jürgen Leeb, and Dr. Andreas Polzer. The longest cooperation exists with XFAB Semiconductor Foundry, and I would like to thank Wolfgang Einbrodt, Dr. Konrad Bach, Detlev Sommer, Dr. Alexander Zimmer, and Dr. Daniel Gäbler for enabling the huge progress with silicon OEICs.

I also warmly thank the project partners from the European projects INSPIRED (Dr. Gernot Langguth and Dr. Holger Wille, Infineon Munich; Dr. Johannes Sturm, Infineon Villach), HELIOS (Dr. Jean-Marc Fedeli, CEA LETI, Grenoble; Dr. Franz Schrank, AMS AG, Premstätten), and IRIS (Francesco Testa, Ericsson, Pisa; Prof. Dr. Lorenzo Pavesi, University of Trento; Dr. Claudio Oton, Scuola Superiore Sant' Anna, Pisa; Dr. Christoph Kopp, CEA LETI, Grenoble (I hope the others can excuse that I cannot include all of them here) as well as the national PHELICITI project partners from AIT (Dr. Bernhard Schrenk, Dr. Paul Müllner) and AMS AG (Dr. Jochen Kraft). Without them, many high-level results would not have been generated and could not have been included in this book.

My deepest gratitude, again, is directed to my wife, my daughters Luise and Lina, as well as to my son Frieder, who would have preferred to bike more often together, for their great patience.

Vienna, Austria Horst Zimmermann

Preface to the First Edition

Since the book “Integrated Silicon Optoelectronics” appeared in the “Springer Series in Photonics” in 2000, a whole variety of silicon optoelectronic integrated circuits (SOEICs) have been developed and introduced in many journals and conference proceedings. Therefore, a new book on these new SOEICs collecting and selecting the most interesting ones was highly desirable especially because the main part of “Integrated Silicon Optoelectronics” concentrated on integrated photodetectors. This new book, in contrast, describes considerably more circuits implemented as SOEICs together with the photodetectors.

Many design engineers in semiconductor companies, ASIC and design houses have to design SOEICs, OPTO-ASICs, image sensors or even smart pixel sensors. I also feel that the number of Ph.D. students or diploma workers doing research and development in the field of optoelectronic circuits is constantly growing. This book, therefore, is intended as a second bridge (after “Integrated Silicon Optoelectronics”) between microelectronics and optoelectronics. Usually, optoelectronics plays a minor role in electrical engineering courses at universities. Physicists are taught optics but not very much semiconductor technology and chip design. This book covers the missing information for engineers and physicists who want to know more about integrated optoelectronic circuits (OEICs) in silicon technologies and about their rapidly emerging applications. The low-cost requirement permanently drives and pushes silicon OEICs in contrast to expensive III/V semiconductor receiver OEICs. This book reflects this trend by stressing CMOS OEICs. BiCMOS OEICs with their better performance, however, are also described in detail, since they are still much cheaper than III/V OEICs.

The importance of OEICs is due to the following advantages of monolithic optoelectronic integrated circuits: (i) good immunity against electromagnetic interference (EMI) because of very short interconnects between photodetectors and amplifiers, (ii) reduced chip area due to the elimination of bondpads, (iii) improved reliability due to the elimination of bondpads and bond wires, (iv) cheaper mass

production compared to discrete circuits, wire-bonded circuits, and hybrid integrated circuits, and (v) larger −3 dB bandwidth compared to discrete circuits, wire-bonded circuits, and some hybrid integrated circuits due to the avoidance of parasitic bondpad capacitances.

This book describes the basics and theory of photodetectors in a compact form. The three chapters on integrated photodetectors, thin-film detectors, and SiGe detectors describe the properties of photodiodes, which were implemented in the circuits discussed later in this book. The chapter on design of integrated circuits covers analytical methods for calculating bandwidth. Methods for calculating input and output resistance as well as electronic noise of transimpedance amplifiers were also added. Furthermore, a transmission line approach leading to a new π-model for integrated transimpedance amplifiers was included.

In the last and longest chapter, new concepts for DVD and CD-ROM OEICs and new results on these still economically more important key devices for optical storage systems were included. The state-of-the-art of fiber receiver OEICs was updated, and new market demands like plastic optic fiber receivers and burst-mode optical receivers are covered by the description of these receiver circuits. The key topics systems-on-chip (SoC) and camera-on-chip (CoC) are included. Within CoCs, revolutionary three-dimensional single-chip CMOS cameras are described. Various CMOS and BiCMOS optical sensor chips are introduced. Several innovative smart sensor circuits are highlighted. Furthermore, speed enhancement techniques for fiber receivers and large-area, large-capacitance photodiodes are explained. The general trend toward deep-sub-micrometer analog–digital CMOS SoCs is considered with respect to OEICs. Finally, new optical interconnect and free-space receivers based on the optoelectronic phase-locked loop principle are introduced.

Parts of the book have their origin in the lecture “Optoelectronic integrated circuits” started at Vienna University of Technology in 2001 and in the lecture “Optoelectronics” I had given from 1994 to 1999 at Kiel University. This book, however, dives much deeper into the topic. The possibilities of SOEICs are described thoroughly with respect to circuits, and some new integrated detectors like the innovative so-called spatially modulated light detector and the photonic mixer device (PMD) are added. The newest publications on silicon OEICs up to 2003 are considered.

I would like to thank Prof. Dr.-Ing. P. Seegebrecht from Kiel University, Germany, where I began research and development on silicon OEICs, for the generous possibility to work independently and to acquire the title “habilitatus.” I am also indebted to Prof. Dr. H. Föll, who offered a wafer prober for the characterization of the OEICs. The work of the OEIC group members at Kiel University, A. Ghazi, T. Heide, M. Hohenbild, K. Kieschnick, and G. Volkholz, is highly appreciated. Three students, N. Madeja, F. Sievers, and U. Willecke, carefully performed simulations and measurements. M. Wieseke and F. Wölk helped with the preparation of numerous drawings. Special thanks go to R. Buchner from the Fraunhofer Institute for Solid-State Technology in Munich and H. Pless from Thesys Microelectronics (now Melexis) in Erfurt, Germany, for their engagement in

the fabrication of CMOS OEICs and BiCMOS OEICs, respectively. I gratefully acknowledge the funding of the projects by the German ministry for education, science, research, and technology (BMBF) within the leading project "Optical Storage."

At the Institute for Electrical Measurements and Circuit Design (EMST) at Vienna University of Technology, I would like to thank my colleague and head of the institute Gottfried Magerl for his great support toward a quick start of research. I also have to thank my Ph.D. students M. Förtsch, J. Knorr, F. Schlögl, K. Schneider, and R. Swoboda for their careful design and characterization work. M. Hofer, Ch. Sünder, and J. Wissenwasser drew many new figures. I further have to thank G. Langguth and H. Wille from Infineon Technologies in Munich, Germany, J. Sturm from Infineon Technologies in Villach, Austria, as well as A. Martin from Infineon Technologies in Vienna, Austria, for their support and constructive cooperation. I further acknowledge funding from the European Commission in the project INSPIRED.

I extend my sincere thanks to Dr. Ascheron and his team at Springer for the good cooperation and their technical support with the text processor. My deepest gratitude, however, is directed to my wife and my daughters, Luise and Lina, as well as to my son Frieder, who supported this second book project with their encouragement and patience.

Vienna, Austria Horst Zimmermann

Contents

1 Basics and Theory . . . 1
1.1 Basics of Optical Absorption . . . 1
1.1.1 Photons and Their Properties . . . 1
1.1.2 Optical Absorption of Important Semiconductor Materials . . . 3
1.1.3 Photogeneration . . . 5
1.2 Semiconductor Equations . . . 6
1.3 Important Models for Photodetectors . . . 8
1.3.1 Carrier Drift . . . 9
1.3.2 Carrier Diffusion . . . 13
1.3.3 Quantum Efficiency and Responsivity . . . 16
1.3.4 Equivalent Circuit of a Photodiode . . . 21
References . . . 24

2 Integrated Silicon Photodetectors . . . 25
2.1 Integrated Detectors in Bipolar Technology . . . 25
2.1.1 Bipolar Processes . . . 25
2.1.2 Integrated Detectors in Standard Bipolar Technology . . . 28
2.1.3 Integrated Detectors in Modified Bipolar Technology . . . 31
2.2 CMOS-Integrated Photodetectors . . . 34
2.2.1 One-Well CMOS Processes . . . 34
2.2.2 Twin-Well CMOS Processes . . . 35
2.2.3 Triple-Well CMOS Processes . . . 36
2.2.4 Integrated Detectors in Standard CMOS Processes . . . 37
2.2.5 Spatially-Modulated-Light Detector . . . 42
2.2.6 PIN Photodiode . . . 43
2.2.7 Charge-Coupled-Device Image Sensors . . . 58
2.2.8 Active-Pixel Sensors . . . 62
2.2.9 Amorphous-Silicon Detectors . . . 67
2.2.10 CMOS-Integrated Bipolar Phototransistors . . . 69

2.2.11 Photonic Mixer Device . . . 72
2.2.12 Avalanche Photodiodes . . . 73
2.2.13 Single-Photon Avalanche Diodes . . . 76
2.3 BiCMOS-Integrated Detectors . . . 78
2.3.1 BiCMOS Processes . . . 78
2.3.2 BiCMOS-Integrated Photodiodes . . . 85
References . . . 94

3 Detectors in Thin Crystalline Silicon Films . . . 105
3.1 Photodiodes in Silicon-on-Insulator . . . 105
3.2 Silicon on Sapphire . . . 110
3.3 Polyimide Bonding . . . 111
References . . . 112

4 SiGe Photodetectors . . . 115
4.1 Heteroepitaxial Growth . . . 115
4.2 Absorption Coefficient of SiGe Alloys . . . 116
4.3 SiGe/Si PIN Hetero-Bipolar-Transistor Integration . . . 117
References . . . 119

5 Design of Integrated Optical Receiver Circuits . . . 121
5.1 Circuit Simulators and Transistor Models . . . 121
5.2 Layout and Verification Tools . . . 126
5.3 Design of OEICs . . . 127
5.4 Transimpedance Amplifier . . . 130
5.4.1 Frequency Response . . . 131
5.4.2 Phase and Group Delay . . . 134
5.4.3 Stability and Compensation . . . 137
5.4.4 Bandwidth of Transistor Transimpedance Amplifier Circuit . . . 137
5.4.5 Bandwidth Limit of Integrated Transimpedance Amplifiers . . . 141
5.4.6 New π-Model for Integrated Transimpedance Amplifier . . . 142
5.4.7 Shunt-Shunt Feedback . . . 151
5.4.8 Input and Output Resistance . . . 155
5.4.9 Noise and Sensitivity . . . 157
5.4.10 Poisson Statistics and Quantum Limit . . . 165
References . . . 166

6 Examples of Optoelectronic Integrated Circuits . . . 169
6.1 Digital CMOS Circuits . . . 170
6.1.1 Synchronous Circuits . . . 170
6.1.2 Asynchronous Circuits . . . 175
6.2 Digital BiCMOS Circuits . . . 177

6.3 Laser Driver Circuits 178
6.4 Analog Circuits 181
6.4.1 Bipolar Circuits 181
6.4.2 Two-Dimensional CMOS Imagers 184
6.4.3 Optical Distance Measurement Circuits 194
6.4.4 3D Sensors with Photodiodes in Standard CMOS 198
6.4.5 3D Sensors with PIN Photodiodes 200
6.4.6 3D Sensors with SPADs 204
6.4.7 Smart Pixel Sensors 206
6.4.8 CMOS Optical Sensors 219
6.4.9 BiCMOS Optical Sensors 234
6.4.10 Sensors Using Single-Photon Detection 237
6.4.11 CMOS Circuits for Optical Storage Systems 238
6.4.12 BiCMOS Circuits for Optical Storage Systems 248
6.4.13 Continuous-Mode Fiber Receivers 268
6.4.14 Receiver for Wireless Infrared Communication 312
6.4.15 OWC Receivers and Experiments with Visible Light 320
6.4.16 Hybrid Receivers 333
6.4.17 Speed Enhancement Techniques 335
6.4.18 Plastic-Optical-Fiber Receivers 348
6.4.19 Burst-Mode Optical Receivers 362
6.4.20 Deep-Sub-μm Receivers 366
6.4.21 Receivers Aiming Towards the Quantum Limit 369
6.4.22 Comparison of Fiber Receivers 384
6.4.23 Special Circuits 389
6.5 Summary 393
References 394

7 Circuits for Electronic-Photonic Integration 407
7.1 3D-Integration Technologies 407
7.1.1 Copper Pillar Connection 407
7.1.2 Through Oxide Vias 408
7.1.3 Through Silicon Vias 409
7.2 Optical Switch 409
7.3 Optical Transceiver 420
7.4 Sensor for Optical Tomography 426
7.5 Sensor for 3D Microimaging 429
References 430

Index 435

About the Author

Dr. Horst Zimmermann received the diploma in Physics in 1984 from the University of Bayreuth, Germany, and the Dr.-Ing. degree from the University Erlangen–Nürnberg working at the Fraunhofer Institute for Integrated Circuits (IIS-B), Erlangen, Germany, in 1991. Then, he was an Alexander-von-Humboldt Research Fellow at Duke University, Durham, N.C., working on diffusion in Si, GaAs, and InP until 1992. In 1993, he joined the Chair for Semiconductor Electronics at Kiel University, Kiel, Germany, where he lectured optoelectronics and worked on optoelectronic integration in silicon technology. Since 2000, he is Full Professor for Electronic Circuit Engineering at Vienna University of Technology, Vienna, Austria. His main interests are in design and characterization of analog and nanometer CMOS circuits as well as optoelectronic integrated CMOS and BiCMOS circuits. He is Author of the Springer books *Integrated Silicon Optoelectronics* and *Silicon Optoelectronic Integrated Circuits* as well as Co-author of *Highly Sensitive Optical Receivers*, *Optical Communication Over Plastic Optical Fibers*, *Analog Filters in Nanometer CMOS*, *Comparators in Nanometer CMOS Technology*, and *Optoelectronic Circuits in Nanometer CMOS Technology*. In addition, he is author and co-author of more than 500 publications. In 2002, he became Senior Member IEEE. He was primary Guest Editor of the November/December 2014 issue of IEEE Journal of Selected Topics in Quantum Electronics on *Optical Detectors: Technology and Applications*.

Symbols

A	Area (cm^2)
A_0	Low-frequency open-loop gain
$A(\omega)$	Frequency-dependent gain
APD	Avalanche photodiode
APP	Afterpulsing probability
c	Speed of light in a medium (cm/s)
c_0	Speed of light in vacuum (cm/s)
c_{bd}	Small-signal bulk-drain capacitance (F)
c_{bs}	Small-signal bulk-source capacitance (F)
c_{cs}	Small-signal collector-substrate capacitance (F)
c_{gb}	Small-signal gate-bulk capacitance (F)
c_{gd}	Small-signal gate–drain capacitance (F)
c_{gs}	Small-signal gate–source capacitance (F)
C_{ox}	Gate-oxide capacitance per area (F)
c_{ws}	Small-signal well-substrate capacitance (F)
c_{je}	Small-signal emitter–base capacitance (F)
c_{μ}	Small-signal base–collector capacitance (F)
C_e	Doping concentration of epitaxial layer (cm^{-3})
C_B	Capacitance of bondpad (F)
C_{BE}	Base–emitter capacitance (F)
C_C	Base–collector space charge capacitance (F)
C_D	Depletion capacitance of photodiode (F)
C_E	Total base–emitter capacitance of bipolar transistor (F)
C_F	Feedback capacitance of transimpedance amplifier (F)
C_{GS}	Gate–source capacitance (F)
C_I	Input capacitance of amplifier (F)
C_L	Load capacitor (F)
C_P	Capacitance of chip package (F)
C_{R_F}	Parasitic capacitance of feedback resistor (F)
C_S	Parasitic capacitance of signal line (F)

C_{SE}	Base–emitter space charge capacitance (F)
C_T	Input node capacitance (F)
d	Distance (m)
d_e	Thickness of epitaxial layer (μm)
d_I	Thickness of intrinsic region (μm)
d_p	Thickness of P-type region (μm)
D	Diffusion coefficient (cm^2/s)
D_n	Diffusion coefficient of electrons (cm^2/s)
D_p	Diffusion coefficient of holes (cm^2/s)
D_t	Decision threshold of photocurrent (A)
DCR	Darc count rate
DR	Data rate (Mb/s)
E_C	Bottom of conduction band (eV)
E_F	Fermi energy level (eV)
E_g	Energy bandgap (eV)
E_t	Energy level of recombination center (eV)
E_V	Top of valence band (eV)
E	Photon energy (eV)
$\boldsymbol{E}$	Electric field (V/cm)
f	Frequency (Hz)
f_g	Bandwidth, −3 dB frequency (Hz)
f_s	Sampling frequency (Hz)
f_T	Transit frequency (gain–bandwidth product) (Hz)
f_{GP}	Frequency of gain peak (Hz)
FF	Fill factor
g_{ds}	Transistor output conductance (A/V)
G	Photogeneration (e-h-p) (cm^{-3}/s)
$G(\omega)$	Frequency response function (V/A)
g_m	Transconductance (A/V)
h	Planck constant (Js)
$\hbar$	$h/2\pi$ (Js)
hv	Photon energy (eV)
i_L	Leakage current of photodiode (A)
I	Current (A)
I_{ph}	Photocurrent (A)
I_{th}	Threshold current (A)
I_B	Base current (A)
I_C	Collector current (A)
I_D	Drain current (A)
I_E	Emitter current (A)
I_S	Source current (A)
$I(x)$	Light intensity distribution (W/m^2)
$I_{i,j}$	Local luminance at pixel (i, j) (W/m^2)
j	Current density (A/cm^2)

k_B	Boltzmann constant (J/K)
$k_B T$	Thermal energy (eV)
L	Length (μm)
L_n	Diffusion length of electrons (μm)
L_p	Diffusion length of holes (μm)
L_B	Inductance of bond wire (H)
L_G	Gate length (μm)
L_W	Inductance of lead wire (H)
$\bar{n}$	Refractive index
$\bar{n}_s$	Refractive index of surroundings
$\bar{n}_{sc}$	Refractive index of semiconductor
$\bar{n}_{ARC}$	Refractive index of antireflection coating
n	Density of free electrons (cm^{-3})
n_i	Intrinsic carrier density (cm^{-3})
N	Impurity concentration (cm^{-3})
N_A	Acceptor concentration (cm^{-3})
N_D	Donor concentration (cm^{-3})
N_t	Concentration of recombination centers (cm^{-3})
p	Density of free holes (cm^{-3})
Q_E	Minority-carrier charge in the base (As)
Q_{pix}	Charge on pixel storage capacitor (As)
QE	Quantum efficiency (%)
P_{opt}	Incident optical power (W)
P_{opt}^{av}	Average incident optical power (W)
$\bar{P}$	Optical power in a semiconductor (W)
PDP	Photon detection probability
q	Magnitude of electronic charge (As)
r_b	Base series resistance (Ω)
r_o	Small-signal output resistance (Ω)
r_c	Small-signal collector series resistance (Ω)
r_{ex}	Small-signal emitter series resistance (Ω)
r_d	Small-signal drain series resistance (Ω)
r_s	Small-signal source series resistance (Ω)
R	Responsivity (A/W)
R_{bb}	Responsivity to black-body radiation (A/W)
R_{ov}	Oversampling ratio
R_D	Parallel resistance (Ω)
R_F	Feedback resistance (Ω)
R_S	Series resistance (Ω)
R_I	Input resistance of amplifier (Ω)
R_L	Load resistance (Ω)
$\bar{R}$	Reflectivity
S	Sensitivity of DVD OEICs (mV/μW)
SPAD	Single-photon avalanche diode

t	Time (s)
t_{d}	Drift time (s)
t_{diff}	Diffusion time (s)
t_{f}	Fall time (s)
t_{int}	Integration time (s)
t_{r}	Rise time (s)
t_{gd}	Group delay (s)
T	Absolute temperature (K)
T_{s}	Sampling time (s)
U	Voltage (V)
U_{BE}	Base–emitter voltage (V)
U_{D}	Built-in voltage (V)
U_{DS}	Drain–source voltage (V)
U_{Ea}	Early voltage (V)
U_{GS}	Gate–source voltage (V)
U_{T}	Thermal voltage k_BT/q (V)
U_{th}	Thermal generation/recombination rate ($cm^{-3}s^{-1}$)
U_{Th}	Threshold voltage (V)
V_{Th}	Threshold voltage (V)
V_{det}	Detector bias (V)
V_{o}	Output voltage (V)
V_{rev}	Reverse voltage (V)
υ	Carrier velocity (cm/s)
υ_{s}	Saturation velocity (cm/s)
υ_{th}	Thermal velocity (cm/s)
W	Width of space charge region (µm)
W_{B}	Base thickness (µm)
W_{G}	Gate width (µm)
Z_{F}	Feedback impedance of transimpedance amplifier (Ω)
x	x direction (µm)
y	y direction (µm)
α	Absorption coefficient (μm^{-1})
β	Current gain of bipolar transistor
β_{F}	Feedback parameter of transimpedance amplifier (Ω^{-1})
η_{e}	External (total) quantum efficiency (%)
η_{i}	Internal quantum efficiency (%)
η_{o}	Optical quantum efficiency (%)
η_{tia}	Efficiency of transimpedance amplifier
$\eta_{\mathrm{tia}}^{bip}$	Efficiency of bipolar transimpedance amplifier
$\eta_{\mathrm{tia}}^{MOS}$	Efficiency of MOS transimpedance amplifier
ϵ_0	Permittivity in vacuum (F/cm)
ϵ_{r}	Relative permittivity
ϵ_{s}	Semiconductor permittivity (F/cm)
$\bar{\epsilon}$	Dielectric function

σ	Carrier capture cross section (cm^{-2})
τ	Lifetime (s)
τ_n	Electron lifetime (s)
τ_p	Hole lifetime (s)
τ_B	Base transit time (s)
$\bar{\kappa}$	Extinction coefficient
λ	Wavelength in a medium (nm)
λ_0	Wavelength in vacuum (nm)
λ_c	Wavelength corresponding to E_g (nm)
λ_{ch}	Channel length modulation parameter (V^{-1})
v	Frequency of light (Hz)
μ	Mobility (cm^2/Vs)
μ_n	Electron mobility (cm^2/Vs)
μ_p	Hole mobility (cm^2/Vs)
ω	Angular frequency (s^{-1})
ω_c	$2 \cdot \pi \cdot f_g$ (s^{-1})
ω_T	$2 \cdot \pi \cdot f_T$ (s^{-1})
ω_{GP}	$2 \cdot \pi \cdot f_{GP}$ (s^{-1})
ρ	Charge density (As/cm^3)
Φ	Photon flux density ($cm^{-2}s^{-1}$)
Ψ	Potential (V)
Θ	Angle ($^\circ$)

Chapter 1
Basics and Theory

Optical absorption is a fundamental process which is exploited when optical energy is converted into electrical energy. Optoelectronic receivers are based on this energy conversion process. Photodetectors convert optical energy into electrical energy. In this chapter, the most important factors needed for the comprehension of photodetectors will be summarized in a compact form. For a detailed description of the basics of optical absorption, the book [1] can be recommended. Here, emphasis will, of course, be placed on silicon devices. After the collection of the most important optical and optoelectronic definitions, we will summarize the fundamentals of device physics and modeling of solid-state electron devices including photodetectors in a compact form. A detailed review on modeling of solid-state electron devices can be found in [2]. Here, the semiconductor equations with implemented photogeneration and the models for carrier mobility used in device simulators will be listed first. Carrier drift and diffusion as well as their consequences for the speed and the quantum efficiency of photodetectors will be explained. Furthermore, the equivalent circuit of a photodiode will be discussed in order to show further aspects concerning the speed of photoreceivers.

First, however, we will introduce photons and the properties of light. Photogeneration will be defined. Furthermore, optical reflection and its consequences on the efficiency of photodetectors will be described.

1.1 Basics of Optical Absorption

1.1.1 Photons and Their Properties

Due to the work of Max Planck and Albert Einstein it is possible to describe light not only by a wave formalism but also by a quantum-mechanical particle formalism.

© Springer Nature Switzerland AG 2018

H. Zimmermann, *Silicon Optoelectronic Integrated Circuits*, Springer Series in Advanced Microelectronics 13, https://doi.org/10.1007/978-3-030-05822-7_1

The smallest unit of light is a quantum-mechanical particle called a photon. The photon, consequently, is the smallest unit of an optical signal. Photons are used to characterize electromagnetic radiation in the optical range from the far infrared to the extreme ultraviolet spectrum. The velocity of photons c in a medium with an optical index of refraction $\bar{n}$ is

$$c = \frac{c_0}{\bar{n}}, \tag{1.1}$$

where c_0 is the velocity of light in vacuum. Photons do not possess a quiescent mass and, unfortunately for the construction of purely optical computers, cannot be stored. Photons can be characterized by their frequency ν and by their wavelength λ:

$$\lambda = \frac{c}{\nu}. \tag{1.2}$$

The frequency of a photon is the same in vacuum and in a medium with index of refraction $\bar{n}$ ($\bar{n} = 1$ for vacuum, $\bar{n} > 1$ in a medium). The wavelength λ in a medium, therefore, is shorter than the vacuum wavelength λ_0 ($\lambda = \lambda_0/\bar{n}$). As a consequence, the vacuum wavelength is used to characterize light sources like light-emitting diodes (LEDs) or semiconductor lasers, because it is independent of the medium in which the light propagates.

Photons can also be characterized by their energy E (h is Planck's constant):

$$E = h\nu = \frac{hc}{\lambda} = \frac{hc_0}{\lambda_0}. \tag{1.3}$$

According to fundamental absorption, this formula leads to the boundary wavelength, which can be detected with the bandgap $E_g = 1.1\,\text{eV}$ of silicon:

$$\lambda_c = \frac{hc_0}{E_g} = 1110\,\text{nm}. \tag{1.4}$$

Only light with shorter wavelengths than 1110 nm can be detected with silicon photodiodes.

A useful relation is given next which allows a quick calculation of the energy for a certain wavelength and vice versa:

$$E = \frac{1240}{\lambda_0} \tag{1.5}$$

where E is in eV and λ_0 in nm. Let us define the flux density Φ as the number of photons incident per time interval on an area A. The optical power P_{opt} incident on a detector with a light sensitive area A, then, is determined by the photon energy and by the flux density:

$$P_{opt} = E\Phi A = h\nu\Phi A. \tag{1.6}$$

Receivers for optical communication or data transmission are characterized by the average optical power P_{opt}^{av} needed to achieve a certain bit error ratio.

1.1.2 Optical Absorption of Important Semiconductor Materials

The energy of a photon can be transferred to an electron in the valence band of a semiconductor, which is brought to the conduction band, when the photon energy is larger than the bandgap energy E_{g}. The photon is absorbed during this process and an electron–hole pair is generated. Photons with an energy smaller than E_{g}, however, cannot be absorbed and the semiconductor is transparent for light with wavelengths longer than $\lambda_{\mathrm{c}} = hc_0/E_{\mathrm{g}}$.

The optical absorption coefficient α is the most important optical constant for photodetectors. The absorption of photons in a photodetector to produce carrier pairs and thus a photocurrent, depends on the absorption coefficient α for the light in the semiconductor used to fabricate the detector. The absorption coefficient determines the penetration depth $1/\alpha$ of the light in the semiconductor material according to Lambert–Beer's law:

$$I(\bar{y}) = I_0 \exp(-\alpha \bar{y}). \tag{1.7}$$

The optical absorption coefficients for the most important semiconductor materials are compared in Fig. 1.1. The absorption coefficients strongly depend on the wavelength of the light. For wavelengths shorter than λ_{c}, which corresponds to the bandgap energy ($\lambda_{\mathrm{c}} = hc_0/E_{\mathrm{g}}$), the absorption coefficients increase rapidly according to the so-called *fundamental absorption*. The steepness of the onset of absorption depends on the kind of band–band transition. This steepness is large for direct band–band transitions as in GaAs ($E_{\mathrm{g}}^{\mathrm{dir}} = 1.42\,\mathrm{eV}$ at 300 K), in InP ($E_{\mathrm{g}}^{\mathrm{dir}} = 1.35\,\mathrm{eV}$ at 300 K), in Ge ($E_{\mathrm{g}}^{\mathrm{dir}} = 0.81\,\mathrm{eV}$ at 300 K) and in $\mathrm{In_{0.53}Ga_{0.47}As}$ ($E_{\mathrm{g}}^{\mathrm{dir}} = 0.75\,\mathrm{eV}$ at 300 K). For Si ($E_{\mathrm{g}}^{\mathrm{ind}} = 1.12\,\mathrm{eV}$ at 300 K), for Ge ($E_{\mathrm{g}}^{\mathrm{ind}} = 0.67\,\mathrm{eV}$ at 300 K) and for the wide bandgap material 6H-SiC ($E_{\mathrm{g}}^{\mathrm{ind}} = 3.03\,\mathrm{eV}$ at 300 K) the steepness of the onset of absorption is small.

$\mathrm{In_{0.53}Ga_{0.47}As}$ and Ge cover the widest wavelength range including the wavelengths 1.3 and 1.54 μm which are used for long distance optical data transmission via optical fibers. The absorption coefficients of GaAs and InP are high in the visible spectrum (≈400–700 nm). Silicon detectors are also appropriate for the visible and near infrared spectral range. The absorption coefficient of Si, however, is one to two orders of magnitude lower than that of the direct semiconductors in this spectral range. For Si detectors, therefore, a much thicker absorption zone is needed than for the direct semiconductors. We will, however, see in this work that with silicon photodiodes GHz operation is nevertheless possible. Silicon is the economically most important semiconductor and it is worthwhile to investigate silicon

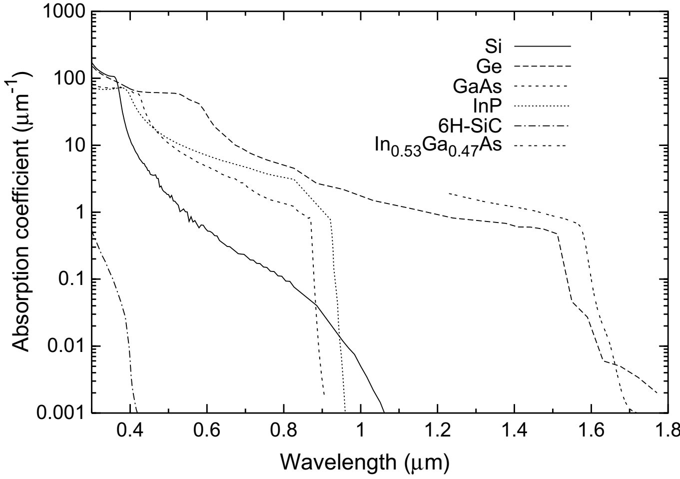

Fig. 1.1 Absorption coefficients of important semiconductor materials versus wavelength

Table 1.1 Absorption coefficients α of silicon and intensity factors I_0 (ehp/cm^3 means electron–hole pairs/cm^3) for several important wavelengths for a constant photon flux density of $\Phi = I_0/\alpha = 1.58 \times 10^{18}$ photons/cm^2

Wavelength (nm)	α (µm^{-1})	I_0 (ehp/cm^3)
850	0.06	9.50×10^{20}
780	0.12	1.89×10^{21}
680	0.24	3.79×10^{21}
635	0.38	6.00×10^{21}
430	5.7	9.00×10^{22}

optoelectronic devices and integrated circuits in spite of the nonoptimum optical absorption of silicon.

The absorption coefficients of silicon for wavelengths which are the most important ones in practice are listed in Table 1.1 [3, 4]. In order to compare the quantum efficiencies of photodetectors for different wavelengths, it is advantageous to use the same photon flux for the different wavelengths. The photocurrents of photodetectors are equal for the same fluxes of photons with different energy, i.e. for different light wavelengths, when the quantum efficiency of the photodetector is the same for the different photon energies or wavelengths, respectively. According to the Lambert–Beer law, different intensity factors I_0 result for a constant photon flux. As an example, intensity factors are listed for the most important wavelengths in Table 1.1 for a certain arbitrary photon flux density.

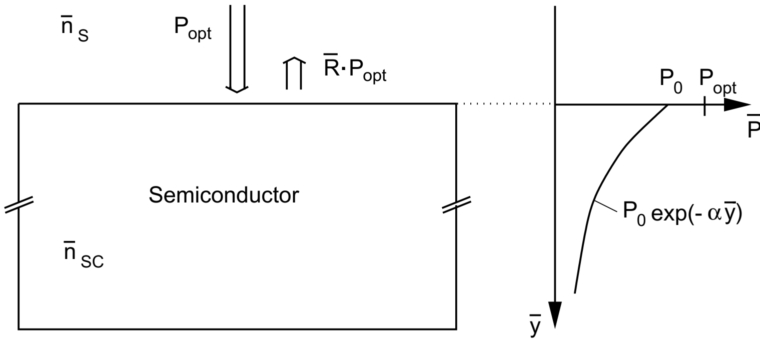

Fig. 1.2 Reflection at a semiconductor surface and decay of the optical power in the semiconductor ($P_0 = (1 - \bar{R})P_{\text{opt}}$)

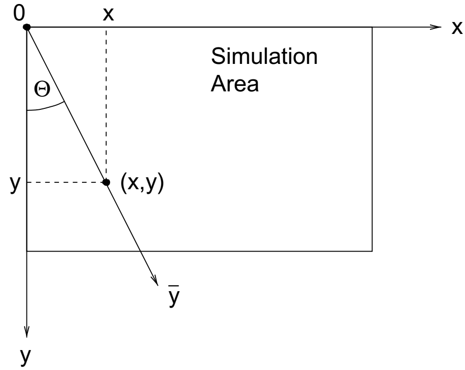

Fig. 1.3 Coordinate transformation from the penetration coordinate $\bar{y}$ to the coordinates (x, y) used in the two-dimensional device simulator for nonperpendicular light incidence

1.1.3 *Photogeneration*

The Lambert–Beer law can be formulated for the optical power $\bar{P}$ analogously to (1.7):

$$\bar{P}(\bar{y}) = P_0 \exp(-\alpha \bar{y}). \tag{1.8}$$

The optical power at the surface of the semiconductor $\bar{P}(\bar{y} = 0)$ is $P_0 = (1 - \bar{R})$ (see Fig. 1.2). The optical power of the light penetrating into a medium decreases exponentially with the penetration coordinate $\bar{y}$ in the medium (compare Fig. 1.3).

The absorbed light generates electron–hole pairs in a semiconductor due to the internal photoeffect provided that $h\nu > E_{\text{g}}$. Therefore, we can express the generation rate per volume $G(\bar{y})$ as:

$$G(\bar{y}) = \frac{\bar{P}(\bar{y}) - \bar{P}(\bar{y} + \triangle\bar{y})}{\triangle\bar{y}} \frac{1}{Ah\nu}. \tag{1.9}$$

In this equation, A is the area of the cross section for the light incidence and $h\nu$ is the photon energy. For $\triangle\bar{y} \to 0$, we can write $(\bar{P}(\bar{y}) - \bar{P}(\bar{y} + \triangle\bar{y}))/\triangle\bar{y} = -\mathrm{d}\bar{P}(\bar{y})/\mathrm{d}\bar{y}$. From (1.8), $\mathrm{d}\bar{P}(\bar{y})/\mathrm{d}\bar{y} = -\alpha\bar{P}(\bar{y})$ then follows and the generation rate is

$$G(\bar{y}) = \frac{\alpha P_0}{Ah\nu}\exp(-\alpha\bar{y}). \tag{1.10}$$

1.2 Semiconductor Equations

The physics of semiconductor devices like diodes, MOSFETs (Metal-Oxide-Silicon Field-Effect Transistors), bipolar transistors, and photodetectors is well known. The equations describing the behavior of these devices in most important cases are the semiconductor equations. These equations have already been implemented in many device simulation programs. The physical models for the parameters used in the semiconductor equations were discussed thoroughly, for instance, in [2].

Device simulation programs have been valuable tools for the development of semiconductor devices for many years. Much time and money can be saved with their help for such a purpose. They are also valuable for the development of photodetectors. We will take the two-dimensional device simulator MEDICI as an example [5]. The drift-diffusion model is implemented in this simulator. MEDICI solves the Poisson equation (1.11), the transport equations (1.13) and (1.14), and the continuity equations (1.16) and (1.17) for electrons and holes. Furthermore, photogeneration is implemented. Due to the photogeneration for the internal photoeffect, electron–hole pairs are created, i.e. the corresponding generation terms for electrons and holes are equal.

The potential Ψ in the device, for which the simulation is performed, is calculated according to the Poisson equation:

$$\triangle\Psi = -\frac{\rho}{\epsilon}\,. \tag{1.11}$$

The quantity ϵ is the product of the relative and absolute dielectric constants: $\epsilon = \epsilon_\mathrm{r}\epsilon_0$. The symbol ρ represents the charge density, which can be further broken apart into the product of the elementary charge q times the sum of the hole concentration p (positively charged), of the electron concentration n (negatively charged), of the donor concentration N_D (positively charged), and of the acceptor concentration N_A (negatively charged):

$$\rho = q(p - n + N_\mathrm{D} - N_\mathrm{A}). \tag{1.12}$$

The current densities for electrons and holes are the sum of the drift and diffusion current densities:

$$\boldsymbol{j}_\mathrm{n} = qn\mu_\mathrm{n}\boldsymbol{E} + qD_\mathrm{n}\,\mathbf{grad}\,n, \tag{1.13}$$

$$\boldsymbol{j}_\mathrm{p} = qp\mu_\mathrm{p}\boldsymbol{E} - qD_\mathrm{p}\,\mathbf{grad}\,p. \tag{1.14}$$

The total current density results from the electron and hole current densities:

$$\boldsymbol{j} = \boldsymbol{j}_\mathrm{n} + \boldsymbol{j}_\mathrm{p}. \tag{1.15}$$

The continuity equations with the inclusion of photogeneration $G(x, y)$ due to the penetration of light into the semiconductor can be written as:

$$\frac{\partial n}{\partial t} = \frac{\mathrm{div}\,\boldsymbol{j}_\mathrm{n}}{q} + U_\mathrm{th} + G(x, y), \tag{1.16}$$

$$\frac{\partial p}{\partial t} = -\frac{\mathrm{div}\,\boldsymbol{j}_\mathrm{p}}{q} + U_\mathrm{th} + G(x, y). \tag{1.17}$$

U_th is the thermal generation/recombination term. The photogeneration $G(\bar{y})$ was derived above. The simulator allows us to define nonperpendicular incidence for the light. Then, $G(x, y) = G(\bar{y} = (x^2 + y^2)^{1/2})$ has to be used (compare with Fig. 1.3).

The electric field is determined by (1.11) and obeys:

$$\boldsymbol{E} = -\mathbf{grad}\,\Psi. \tag{1.18}$$

The electric field, for instance, is important for the calculation of the drift velocity $\boldsymbol{v}$ of photogenerated carriers in photodetectors:

$$\boldsymbol{v} = \mu\boldsymbol{E}. \tag{1.19}$$

The mobilities of electrons and holes differ strongly and μ_n or μ_p has to be used for μ in order to calculate the electron drift velocity or the hole drift velocity, respectively. The mobilities μ_n and μ_p are only constant for a low electric field. It will be shown below that the drift velocities of electrons and holes saturate for large values of the electric field.

For the calculation of the speed of photodetectors we not only need the mobilities and the electric field but also the width of the space-charge region, where an electric field is present. In the so-called depletion approximation, i.e. with n and p approximately equal to zero in the space-charge region and $\rho = 0$ outside the space-charge region, the distribution of the electric field and the width of the space-charge region W can be calculated analytically for an abrupt PN junction:

$$W = \sqrt{\frac{2\epsilon_\mathrm{r}\epsilon_0}{q}\frac{N_\mathrm{A} + N_\mathrm{D}}{N_\mathrm{A}N_\mathrm{D}}\left(U_\mathrm{D} - U - \frac{2k_\mathrm{B}T}{q}\right)}, \tag{1.20}$$

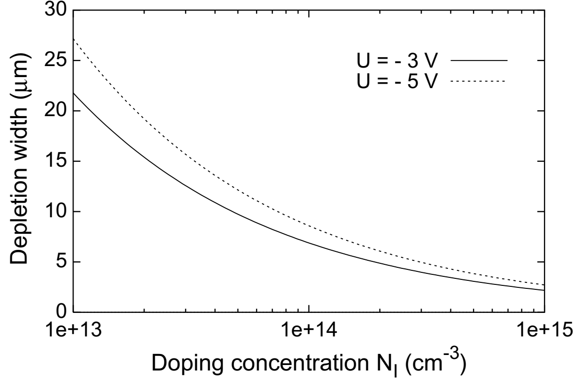

Fig. 1.4 Depletion layer width versus doping concentration of the lower doped side of a PN junction

with

$$U_{\mathrm{D}} = \frac{k_{\mathrm{B}}T}{q} \ln \frac{N_{\mathrm{A}}N_{\mathrm{D}}}{n_{\mathrm{i}}^2}. \tag{1.21}$$

Let us assume that one side of the PN junction is doped to a much larger extent than the other, for instance $N_{\mathrm{D}} = 10^{20}\,\mathrm{cm}^{-3} \gg N_{\mathrm{A}} = 10^{16}\,\mathrm{cm}^{-3}$ or vice versa. We want to define the lower doping concentration as N_{I}. Equation (1.20) then can be simplified to

$$W = \sqrt{\frac{2\epsilon_{\mathrm{r}}\epsilon_0}{qN_{\mathrm{I}}}\left(U_{\mathrm{D}} - U - \frac{2k_{\mathrm{B}}T}{q}\right)}. \tag{1.22}$$

For the reverse voltage U, here, a negative value always has to be used. The space-charge region only spreads into the low doped side of the PN junction due to the simplification. This behavior, however, is a good approximation for most semiconductor diodes and for photodiodes, accordingly. The width of the space-charge region as a function of the doping concentration of the low doped side of the PN junction is shown in Fig. 1.4.

1.3 Important Models for Photodetectors

The most important processes for the characterization of photodetectors with respect to their speed are carrier drift and minority carrier diffusion. The carrier drift in conventional semiconductor materials is a much faster process than the minority carrier diffusion. For the calculation of the frequency response of photodiodes, series resistances and PN junction capacitances are also important. An even more complete equivalent circuit for photodiodes considering wiring capacitances will be discussed. Minority carrier diffusion, series resistances and capacitances reduce the speed of photodiodes.

Table 1.2 Parameter values for the approximation of the electron and hole mobilities in silicon with (1.23) and (1.24)

Parameter	Electrons	Holes
μ_{min} (cm^2/Vs)	17.8	48.0
μ_{max} (cm^2/Vs)	1350	495
N_{ref} (cm^{-3})	1.072×10^{17}	1.606×10^{17}
$\nu_{\text{n,p}}$	−2.3	−2.2
$\chi_{\text{n,p}}$	−3.8	−3.7
$\alpha_{\text{n,p}}$	0.73	0.70

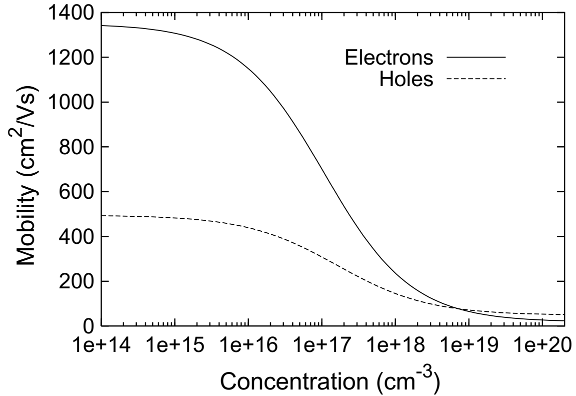

Fig. 1.5 Carrier mobilities in silicon versus total doping concentration [6, 7]

1.3.1 *Carrier Drift*

The carrier mobilities in the drift terms (see (1.13) and (1.14)) are the parameters which are responsible for the obtainable speed of photodetectors. The carrier mobilities depend on the doping concentration and on the electric field. An empirical expression is available for the dependence of the mobility on the total impurity concentration N_{total}, which also considers the influence of temperature T in K [6, 7]:

$$\mu_{0\text{n}} = \mu_{\text{n,min}} + \frac{\mu_{\text{n,max}} (T/300)^{\nu_\text{n}} - \mu_{\text{n,min}}}{1 + (T/300)^{\chi_\text{n}} (N_{\text{total}}/N_{\text{ref,n}})^{\alpha_\text{n}}}, \tag{1.23}$$

$$\mu_{0\text{p}} = \mu_{\text{p,min}} + \frac{\mu_{\text{p,max}} (T/300)^{\nu_\text{p}} - \mu_{\text{p,min}}}{1 + (T/300)^{\chi_\text{p}} (N_{\text{total}}/N_{\text{ref,p}})^{\alpha_\text{p}}}. \tag{1.24}$$

N_{total} is the sum of the concentrations of acceptors and donors. The other parameters for silicon are listed in Table 1.2.

The dependence of the carrier mobilities in silicon on the doping concentration according to (1.23) and (1.24) is shown in Fig. 1.5 for $T = 300$ K.

Fig. 1.6 Carrier mobilities versus electric field for weakly doped silicon

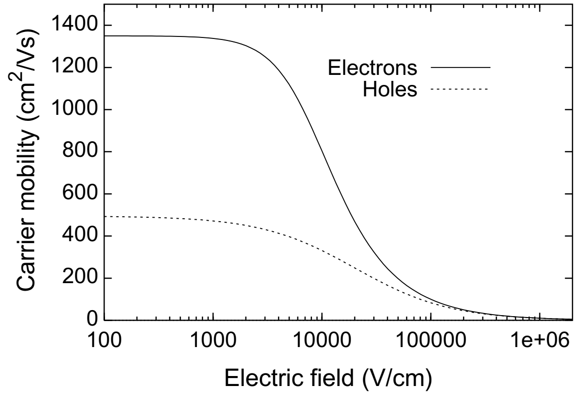

According to [6], the dependence of the carrier mobilities in silicon on the electric field can be approximated by

$$\mu_{\mathrm{n}} = \frac{\mu_{0\mathrm{n}}}{1 + (\mu_{0\mathrm{n}} E / v_{\mathrm{n}}^{\mathrm{sat}})^2}, \tag{1.25}$$

$$\mu_{\mathrm{p}} = \frac{\mu_{0\mathrm{p}}}{1 + (\mu_{0\mathrm{p}} E / v_{\mathrm{p}}^{\mathrm{sat}})^1}. \tag{1.26}$$

The values for the saturation velocities (in cm/s) can be computed from the expression [8] with T in K:

$$v_{\mathrm{n}}^{\mathrm{sat}}(T) = v_{\mathrm{p}}^{\mathrm{sat}}(T) = \frac{2.4 \times 10^7}{1 + 0.8 \exp(T/600)}. \tag{1.27}$$

The curves calculated with (1.25) and (1.26) are shown in Fig. 1.6 for a very low doping concentration, i.e. for the ‘intrinsic’ zone of a PIN photodiode. The carrier mobilities begin to degrade for electric fields in excess of approximately 2000 V/cm.

The drift velocities, therefore, are proportional to the electric field only for smaller values of the electric field (Fig. 1.7). For values of the electric field larger than approximately 10,000 V/cm the electron drift velocity saturates. For holes, the electric field has to exceed a value of approximately 100,000 V/cm in order to obtain the hole saturation velocity.

The dependence of the carrier mobilities on the doping concentration is implemented in MEDICI with the CONMOB model [5]. The model in MEDICI for the dependence of the carrier mobilities, i.e. of the drift velocities on the electric field is called FLDMOB.

One quantity, which should be mentioned here, is the drift time, i.e. the time needed by carriers to drift through the whole width W of the space-charge region or drift zone. The drift time is determined by the drift velocity v and by the width of

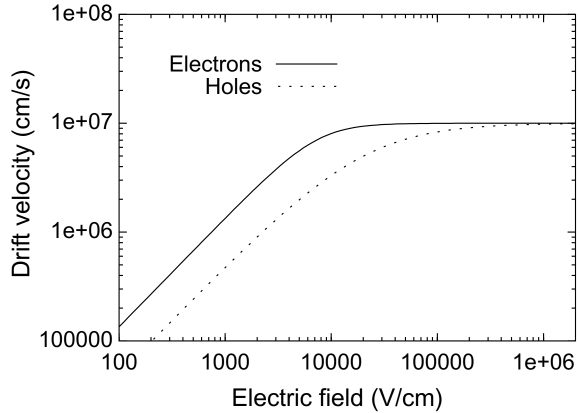

Fig. 1.7 Carrier drift velocities in silicon versus electric field calculated according to (1.19), (1.25) and (1.26) for a low doping concentration

the drift zone W. The drift velocity v depends on μ and E. Furthermore, μ depends on the doping concentration. The doping concentration and the bias voltage applied to the photodiode determine the distribution of the electric field. It is, therefore, very difficult to calculate the drift time analytically, because v, μ and E in a real photodetector depend on the space coordinates. Numerical process and device simulations, in general, are necessary in order to compute the transient response of photodetectors.

When we choose the ideal PIN photodiode with a constant electric field for instance (see Fig. 1.8), it is possible to give some analytical expressions for the drift time t_d and for the rise and fall times t_r and t_f of the photocurrent (time difference between the 10 and 90% values of the stationary photocurrent) [9]:

$$t_\mathrm{d} = t_\mathrm{r} = t_\mathrm{f} = \frac{d_\mathrm{I}}{v(E_0)}. \tag{1.28}$$

Instead of W, the thickness of the intrinsic I-layer of the ideal PIN photodiode d_I is used in (1.28). For a large reverse voltage, which results in a large value of the electric field, the drift velocities may be approximated by the saturation velocity v_s and

$$t_\mathrm{d} = t_\mathrm{r} = t_\mathrm{f} = \frac{d_\mathrm{I}}{v_\mathrm{s}} \tag{1.29}$$

results. The rise and fall times limit the maximum data rate DR of optical receivers. The maximum data rate of a photodiode (in the non-return-to-zero transmission mode) can be estimated in a conservative way to be the lower value of $\mathrm{DR} = 1/(3t_\mathrm{r})$ and $\mathrm{DR} = 1/(3t_\mathrm{f})$. The mean value of t_r and t_f may lead to $\mathrm{DR} = 2/(3(t_\mathrm{r} + t_\mathrm{f}))$. In a more aggressive way, instead of the factor 3, the factor 2 can be used, however, in practice the bit-error rate of optical receivers determines the usable data rate. The relation between the rise time and the $-3\,\mathrm{dB}$ bandwidth should also be mentioned [10, 11]: